Chemistry–A European Journal | Research Article
doi.org/10.1002/chem.202202147
Chemistry Europe
European Chemical Societies Publishing
www.chemeurj.org

Theoretical and Experimental Investigation of Functionalized Cyanopyridines Yield an Anolyte with an Extremely Low Reduction Potential for Nonaqueous Redox Flow Batteries

Thomas P. Vaid[+],[a, b] Monique E. Cook[+],[a, b] Jessica D. Scott,[a, b] Marino Borjesson Carazo,[a, d] Jonathan Ruchti,[a, e] Shelley D. Minteer,[a, e] Matthew S. Sigman,[a, e] Anne J. McNeil,[a, b, c] and Melanie S. Sanford*[a, b]

Abstract: Cyanopyridines and cyanophenylpyridines were investigated as anolytes for nonaqueous redox flow batteries (RFBs). The three isomers of cyanopyridine are reduced at potentials of −2.2 V or lower vs. ferrocene$^{+/0}$ ($Fc^{+/0}$), but the 3-$CNPy^{\bullet-}$ radical anion forms a sigma-dimer that is re-oxidized at $E \approx -1.1$ V, which would lead to poor voltaic efficiency in a RFB. Bulk electrochemical charge-discharge cycling of the cyanopyridines in acetonitrile and 0.50 M $[NBu_4][PF_6]$ shows that 2-CNPy and 4-CNPy lose capacity quickly under these conditions, due to irreversible chemical reaction/decomposition of the radical anions. Density-functional theory (DFT) calculations indicated that adding a phenyl group to the cyanopyridines would, for some isomers, limit dimerization and improve the stability of the radical anions, while shifting their $E_{1/2}$ only about +0.10 V relative to the parent cyanopyridines. Among the cyanophenylpyridines, 3-CN-6-PhPy and 3-CN-4-PhPy are the most promising as anolytes. They exhibit reversible reductions at $E_{1/2} = -2.19$ and −2.22 V vs. ferrocene$^{+/0}$, respectively, and retain about half of their capacity after 30 bulk charge-discharge cycles. An improved version of 3-CN-6-PhPy with three methyl groups (3-cyano-4-methyl-6-(3,5-dimethylphenyl)pyridine) has an extremely low reduction potential of −2.50 V vs. $Fc^{+/0}$ (the lowest reported for a nonaqueous RFB anolyte) and loses only 0.21% of capacity per cycle during charge-discharge cycling in acetonitrile.

Introduction

Redox flow batteries (RFBs) are a promising technology for inexpensive large-scale electrical energy storage.[1–3] Commercial redox flow batteries are based on aqueous solutions containing inorganic redox species such as vanadium, iron, or zinc-bromine.[4] In contrast to those inorganic species, redox-active organic molecules afford the opportunity to modify molecular structure to tune redox potentials, stability, solubility, and other properties.[5,6] For example, we have developed very high-potential thioether-containing cyclopropenium catholytes,[7] derivatized and optimized 4-acylpyridinium cations to improve their cycling stability as anolytes,[8] modified the alkyl substituents on tris(dialkylamino)cyclopropenium cations to improve solubility to over 1 M in CH_3CN,[9] and synthesized tris(dialkylamino)cyclopropenium oligomers with extremely low rates of crossover across the flow battery membrane.[10] Reversible redox of these very high- and low-potential molecules is only possible in organic solvents, which have electrochemical windows as large as 5 V,[11,12] whereas aqueous systems have a window of approximately 1.5 V.

In our search for new redox-active organic molecules for high energy density RFBs, we identified cyanopyridine derivatives as promising candidates. The reductive cyclic voltammetry (CV) of 2-, 3-, and 4-cyanopyridine (2-CNPy, 3-CNPy, and 4-CNPy; Scheme 1a) in several solvents has been reported.[13–18]

[a] Dr. T. P. Vaid,[+] M. E. Cook,[+] J. D. Scott, Dr. M. Borjesson Carazo, Dr. J. Ruchti, Prof. S. D. Minteer, Prof. M. S. Sigman, Prof. A. J. McNeil, Prof. M. S. Sanford
Joint Center for Energy Storage Research
9700 S. Cass Avenue, Argonne, Illinois 60439 (USA)
E-mail: mssanfor@umich.edu
[b] Dr. T. P. Vaid,[+] M. E. Cook,[+] J. D. Scott, Prof. A. J. McNeil, Prof. M. S. Sanford
Department of Chemistry
University of Michigan
930 North University Avenue, Ann Arbor, Michigan 48109 (USA)
[c] Prof. A. J. McNeil
Macromolecular Science and Engineering Program
University of Michigan
Ann Arbor, Michigan 48109 (USA)
[d] Dr. M. Borjesson Carazo
Institute of Chemical Research of Catalonia (ICIQ)
The Barcelona Institute of Science and Technology
Av. Països Catalans 16, 43007 Tarragona (Spain)
[e] Dr. J. Ruchti, Prof. S. D. Minteer, Prof. M. S. Sigman
Department of Chemistry
University of Utah
315 South 1400 East, Salt Lake City, Utah 84112 (USA)
[+] These authors contributed equally to this work.

Supporting information for this article is available on the WWW under https://doi.org/10.1002/chem.202202147

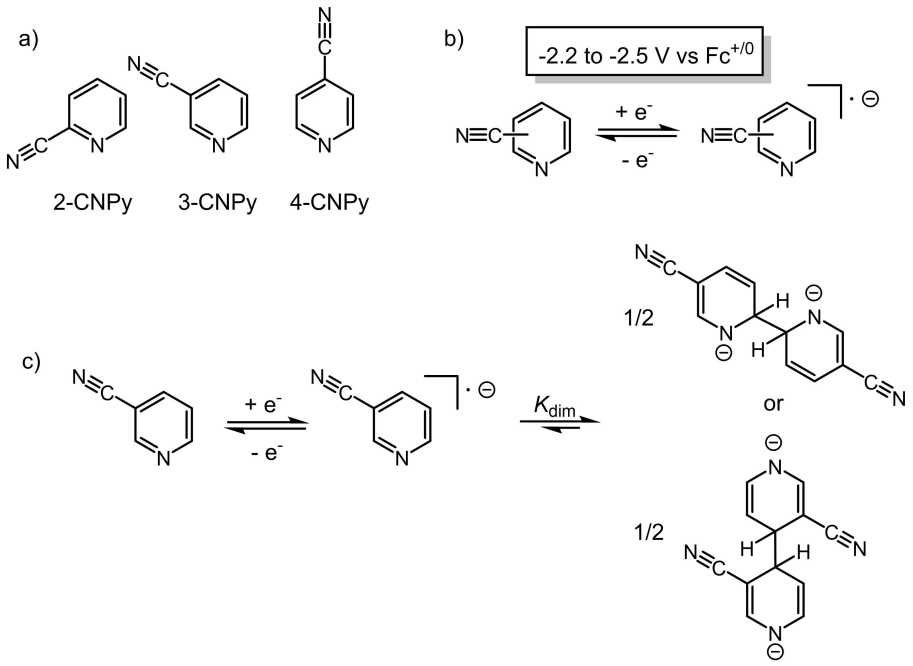

Scheme 1. (a) The three cyanopyridine isomers. (b) Their reduction to the radical anion. (c) Proposed dimerization of the 3-CNPy$^{\bullet-}$ radical anion.

The reduction potential, $E_{1/2}$, for the conversion of the neutral molecules to their radical anions (Scheme 1b) was reported to range from −2.2 to −2.5 V versus $Fc^{+/0}$ (Fc = ferrocene), depending on the isomer, solvent, and supporting electrolyte. These potentials are comparable to the lowest potentials reported for nonaqueous RFB anolytes, such as 2-methylbenzophenone (−2.34 V versus $Fc^{+/0}$).[19] For both 4-CNPy and 2-CNPy, the reduction was reversible in those CV experiments.[14,15] In contrast, for 3-CNPy the radical anion rapidly dimerized to a dianion (at either the 2- or 4-position, Scheme 1c), with an equilibrium constant $K_{dim} = 10^7\ M^{-1}$ in CH_3CN.[18]

Based on these reports of reversible, low-potential reduction, we undertook a detailed study of cyanopyridine derivatives as anolytes for redox flow batteries. Herein we report the cyclic voltammetry and bulk charge-discharge cycling of 2-CNPy, 3-CNPy, and 4-CNPy in a flow battery-relevant medium, CH_3CN with 0.50 M $[NBu_4][PF_6]$ supporting electrolyte. We hypothesized that installing a phenyl substituent on the cyanopyridines would improve the cycling stability of 2-CNPy and 4-CNPy and possibly prevent the dimerization of the 3-CNPy radical anion, while minimally impacting their reduction potentials. We examined all ten isomers of cyanophenylpyridine by density functional theory (DFT) calculations and then experimentally by cyclic voltammetry and bulk charge-discharge cycling. This ultimately revealed 3-CN-6-PhPy to be the optimal cyanophenylpyridine isomer, as it did not dimerize upon reduction and had good capacity retention during cycling. Further improved cycling stability and an even lower reduction potential was achieved by the addition of methyl groups to 3-CN-6-PhPy.

Results and Discussion

Cyanopyridines

The reductive electrochemistry of one or more of the cyanopyridine isomers has been reported in melt,[17] as well as in solutions in water,[13] liquid ammonia,[14] CH_3CN,[15] and DMF.[16,18] We collected the CVs of all three molecules under conditions most relevant to non-aqueous redox flow batteries: in CH_3CN with 0.50 M $[NBu_4][PF_6]$ supporting electrolyte. The CV experiments were conducted with 10 mM cyanopyridine, a glassy carbon (GC) disk working electrode, Pt wire or GC counter electrode, and a Ag/Ag^+ (10 mM $AgBF_4$) reference or Ag wire pseudoreference electrode, with potentials adjusted to $Fc/Fc^+ = 0$ V by adding an internal ferrocene standard for a final voltammogram. Scan rates were 100 mV/s unless noted otherwise.

Under these conditions, 4-CNPy is reduced at $E_{1/2} = -2.23$ V vs. $Fc^{+/0}$ (Figure 1c). There is no discernible re-oxidation peak at higher potential that would indicate dimerization of the radical anion and oxidation of that dianion. However, the ratio of the peak oxidative current to the peak reductive current, i_{pa}/i_{pc}, is only 0.92, possibly due to the formation of a small amount of dimer. For 2-CNPy, the reduction occurs at −2.40 V (Figure 1a), and in this case $i_{pa}/i_{pc} = 0.77$, indicating some reaction or decomposition of the radical anion. The small oxidative peak at approximately −0.9 V is a strong indication of radical anion dimerization (with oxidation of the dianionic dimer to the monomeric neutral molecule occurring at −0.9 V). The $E_{1/2}$ values for reduction of both 4-CNPy and 2-CNPy are within 10 mV of reported values.[14,15,20] In contrast to the CVs of 4-CNPy and 2-CNPy, the CV of 3-CNPy (Figure 1b) shows no return

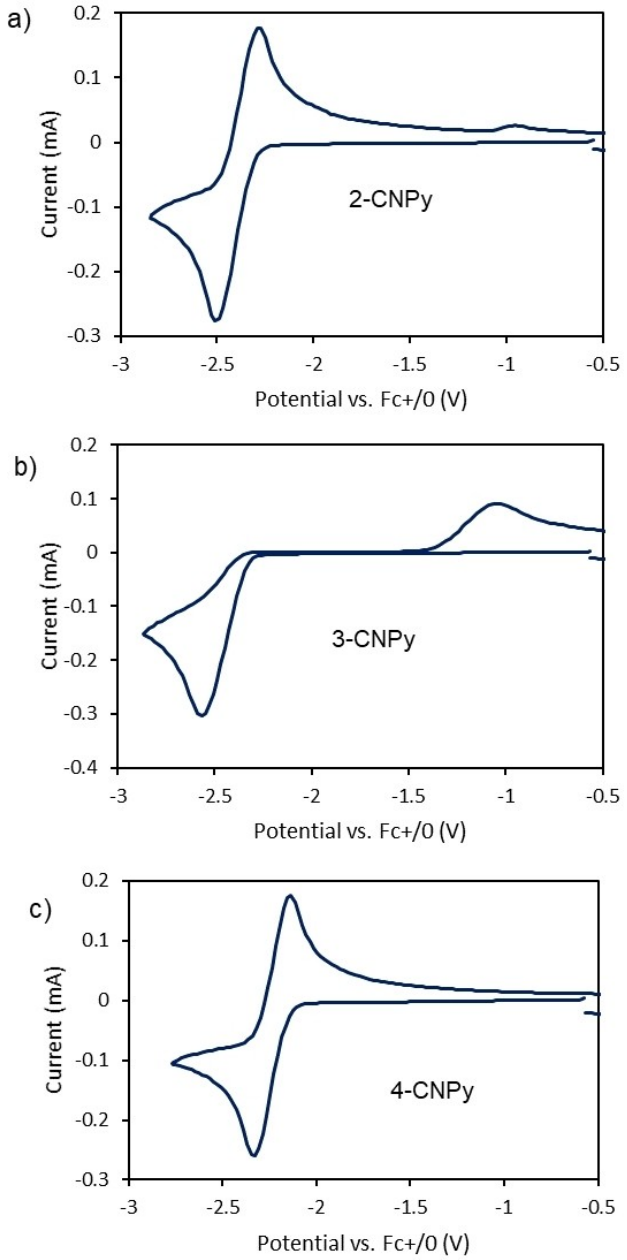

Figure 1. Cyclic voltammograms of 10 mM (a) 2-cyanopyridine, (b) 3-cyanopyridine, and (c) 4-cyanopyridine at a glassy carbon electrode in CH_3CN with 0.50 M $[NBu_4][PF_6]$ at a scan rate of 100 mV/s.

oxidation at the potential near where the radical anion is formed ($E_{p/2} = -2.43$ V vs. $Fc^{+/0}$).[18] (For irreversible processes, the $E_{1/2}$ can be estimated by $E_{p/2}$, the voltage at the point where the current is half of the peak current.) Instead, the anodic peak appears at approximately −1.0 V vs. $Fc^{+/0}$, consistent with the formation and reoxidation of a dimeric dianion.[18] This dimerization is undesirable for a redox flow battery, as the large separation between the anodic and cathodic peaks will result in poor voltaic and energy efficiency during battery cycling.

The cyanopyridine isomers were next subjected to bulk charge-discharge cycling in an H-cell with ultrafine fritted glass separating the two chambers and reticulated vitreous carbon (RVC) electrodes on each side. These experiments were conducted using 5.0 mL of a 5.0 mM solution of the redox active molecule in CH_3CN with 0.50 M $[NBu_4][PF_6]$ supporting electrolyte on each side of the H-cell (with the counter-electrode solution swapped out for fresh solution after the first half-cycle). The bulk cycling experiments were performed several times on each isomer, and a representative run for each is shown in Figure 2. The stability of 4-CNPy during cycling was poor, as it lost 80–100% of its capacity over one charge-discharge cycle and the remainder in the second cycle. The 2-CNPy isomer is slightly more stable, losing 60–90% of its capacity over the first cycle, with complete capacity loss after a few more cycles. Significantly higher stability was exhibited by 3-CNPy, which, after an initial loss of capacity in the first cycle, lost capacity at a rate of 1.3% per cycle. However, 3-CNPy discharged through the dimeric dianion (pictured in Scheme 1c), at a potential of about −1.4 V, and therefore would have poor voltaic efficiency in a battery.

Based on these initial experiments, we sought to design cyanopyridine derivatives that address two problematic features of the parent compounds: (1) their low stability during charge-discharge cycling and (2) their susceptibility to dimerization, which negatively impacts voltaic efficiency. To understand the propensity for dimerization and the relative reduction potentials of the cyanopyridines, hybrid density functional theory (DFT) calculations were performed on 2-, 3-, and 4-cyanopyridine along with their radical anions.

Reduction potentials were calculated using a published method in which the energy of each neutral molecule and its radical anion is calculated (B3LYP/6-311+G**//B3LYP/6-31G*, with a "polar solvent" model) and the energy of the radical anion is subtracted from the energy of the neutral molecule to obtain the electron affinity (using, in all cases, just the "electronic energy" from the calculation). A constant offset of 4.87 V was then subtracted to convert those electron affinities (expressed in eV) to solution-phase reduction potentials versus

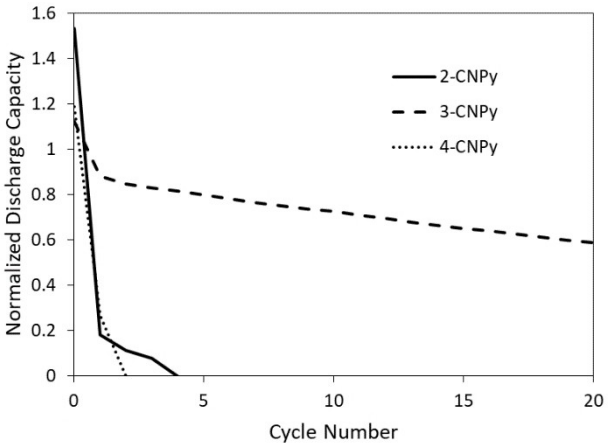

Figure 2. Discharge capacity as a function of cycle number during bulk charge-discharge cycling of 2-, 3-, and 4-cyanopyridine (5.0 mL of a 5.0 mM solution; current = 5.00 mA) in CH_3CN with 0.50 M $[NBu_4][PF_6]$, normalized to a theoretical capacity of 0.67 mAh.

a $Fc^{+/0}$ reference.[21,22] Details are given in the Supporting Information. The calculated redox potentials for these molecules are shown in Table 1. In all cases, the calculated potential is very close (±40 mV) to that observed experimentally.

The calculated Mulliken spin density isosurfaces at each of the carbons of the pyridine ring for the three radical anions are shown in Figure 3. (The calculated values are given in Figure S1 of the Supporting Information.) The highest spin density at any carbon atom among the three isomers is at C-6 of the 3-$CNPy^{\bullet-}$ radical anion (0.445), a site where dimerization has been proposed to occur.[18] In the 2-$CNPy^{\bullet-}$ radical anion, C-5 has a fairly high spin density of 0.326, consistent with the small amount of dimerization observed in the CV of 2-CNPy. Finally, for 4-$CNPy^{\bullet-}$, where little or no dimerization was observed in CV experiments, the highest spin density is 0.197 at C-4, where the cyano group sterically inhibits dimerization.

While the calculated spin densities are consistent with the relative dimerization propensity of the three radical anions, to gain a clearer understanding of the phenomenon we calculated the free energy of dimerization (ΔG_{dim}) for the three radical anions, at multiple sites on each one. The geometry of each radical anion and each dimeric dianion was optimized in the gas phase (B3LYP-D3/6-311++G**) and a vibrational and thermodynamic calculation was performed at the same level and basis set. Then, for each radical anion or dimer, a single-point energy calculation was performed (B3LYP-D3/6-311++G**) with the Spartan C-PCM "polar solvent" model (dielectric constant of 37.22, close to the reported value[23] of 35.9 for CH_3CN at 25 °C), and the solvation energies were used as a correction to the gas-phase calculated free energies. The calculated ΔG_{dim} values in the gas phase and in solution are given in Table 2. Further details concerning the calculations of ΔG_{dim} are given in the Supporting Information.

Table 1. Reduction potentials of cyanopyridines predicted computationally and determined experimentally.

molecule	calculated $E_{1/2}$ (V vs. $Fc^{+/0}$)	experimental $E_{1/2}$ (V vs. $Fc^{+/0}$)
2-cyanopyridine	−2.38	−2.40
3-cyanopyridine	−2.47	−2.43 ($E_{p/2}$)
4-cyanopyridine	−2.20	−2.23

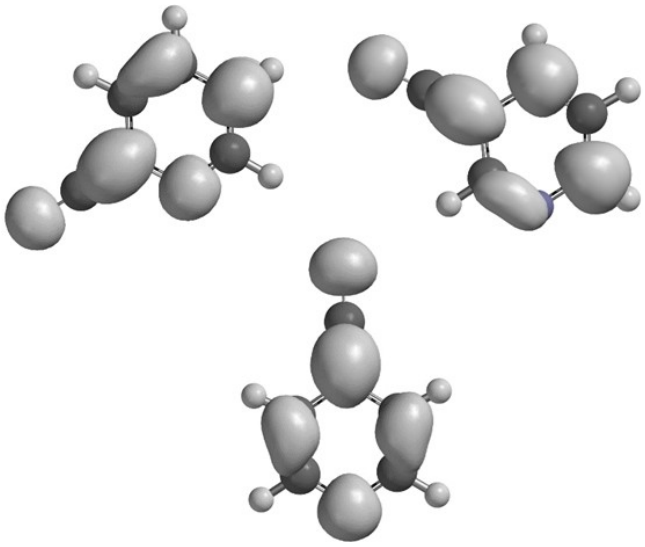

Figure 3. Mulliken spin density isosurfaces for the 2-$CNPy^{\bullet-}$, 3-$CNPy^{\bullet-}$, and 4-$CNPy^{\bullet-}$ radical anions.

In the gas phase, all dimerizations have a large positive ΔG_{dim}, which is unsurprising as dimerization bonds two anions to make a dianion. For all the isomers, the solution-phase ΔG_{dim} is significantly lower than in the gas phase (and in some cases is negative) because in all cases the energy of solvation of the dianion is more than twice that of the radical anion. For 4-$CNPy^{\bullet-}$, the lowest ΔG_{dim} is +18.4 kcal/mol at C-3. There is a higher calculated spin density at C-4, but dimerization is sterically encumbered by the cyano group at that position, as reflected in the calculated bond lengths of the new sigma bond of the dimers: 1.635 Å in the C-4-C-4 dimer and 1.587 Å in the C-3-C-3 dimer. The relatively large, positive ΔG_{dim} is consistent with the lack of dimerization observed in the CV of 4-CNPy. For 2-$CNPy^{\bullet-}$, the most favorable position for dimerization is C-5, which is the carbon atom with the highest calculated spin density. However, the ΔG_{dim} is still positive at +15.9 kcal/mol, so it is somewhat surprising that any dimerization is observed in the CV of 2-CNPy.

For the 3-$CNPy^{\bullet-}$ radical anion, the ΔG_{dim} was calculated for a C-4-C-4 dimer, C-6-C-6 dimer, and a C-4-C-6 cross-dimer. The C-6 dimer was examined in two different rotational geometries around the newly created C-6-C-6 sigma bond, with an *anti* and *gauche* arrangement of the C–H bonds (the *anti* geometry belongs to the C_i point group and the *gauche* to the C_2 point group). While the highest calculated spin density of 3-$CNPy^{\bullet-}$ is at C-6 (and that has been previously suggested to be a site of dimerization[18]), the ΔG_{dim} at C-6 was calculated to be +0.2 kcal/mol (in the gauche configuration). The most favorable dimerization was calculated to be at C-4, with a ΔG_{dim} of −2.0 kcal/mol. The C-4-C-6 cross-dimer gave an intermediate ΔG_{dim} of −1.0 kcal/mol. However, all calculated 3-$CNPy^{\bullet-}$ ΔG_{dim} are within 2.2 kcal/mol of each other, so the calculations do not definitively indicate where dimerization occurs. Furthermore, it seems likely that for all of the isomers the actual ΔG_{dim} under the CV conditions (in 0.50 M $[NBu_4][PF_6]$ in CH_3CN) is lower (more favorable) than the calculated values in Table 2, due to

Table 2. Calculated free fnergies of dimerization of cyanopyridine radical anions.

radical anion	dimerization position	gas-phase dimerization ΔG [kcal/mol]	solution-phase dimerization ΔG [kcal/mol]
2-$CNPy^{\bullet-}$	C-2	85.4	28.5
2-$CNPy^{\bullet-}$	C-5	52.7	15.9
2-$CNPy^{\bullet-}$	C-6	74.2	27.5
3-$CNPy^{\bullet-}$	C-4	52.0	−2.0
3-$CNPy^{\bullet-}$	C-6, anti	43.8	0.9
3-$CNPy^{\bullet-}$	C-6, gauche	48.8	0.2
3-$CNPy^{\bullet-}$	C-4-C-6	45.3	−1.0
4-$CNPy^{\bullet-}$	C-2	80.4	29.6
4-$CNPy^{\bullet-}$	C-3	70.4	18.4
4-$CNPy^{\bullet-}$	C-4	84.5	27.8

stabilization of the dianionic dimers by ion pairing with the NBu_4^+ cations of the supporting electrolyte (which are not present in the calculations). Thus, the dimer is found experimentally to be highly favored for 3-CNPy$^{\bullet-}$ (in contrast to the calculated ΔG_{dim} near zero) and dimerization is only somewhat disfavored for 2-CNPy$^{\bullet-}$ (in contrast to the calculated $\Delta G_{dim} = +$ 15.9 kcal/mol).

Cyanophenylpyridines

The cyanopyridines either had low stability during bulk charge-discharge cycling (2-CNPy and 4-CNPy) or the radical anion dimerized, resulting in a discharge potential that would yield a low voltaic efficiency in a battery (3-CNPy). We hypothesized that adding a phenyl substituent to the cyanopyridines would stabilize the radical anions due to spin delocalization, sterically limit dimerization and decomposition pathways without significantly affecting the reduction potentials. We computationally predicted the reduction potentials for all ten possible isomers of cyanophenylpyridine as well as the free energy of dimerization of the four isomers of 3-CN-x-PhPy. All ten isomers were also examined experimentally by CV and bulk charge-discharge cycling.

DFT Calculations of Reduction Potentials and Dimerization Free Energies

The reduction potentials for the ten cyanophenylpyridine isomers were calculated using DFT in the same way as described above for the cyanopyridines, with the same adjustment of 4.87 V to give a reduction potential versus a ferrocene reference, yielding the values in Figure 4. The computations predict that adding a phenyl group will result in essentially no change in $E_{1/2}$ for two of the molecules (2-CN-6-PhPy and 3-CN-5-PhPy, both with a *meta* relative arrangement of the CN and Ph groups) up to a shift of +0.24 V for 3-CN-6-PhPy (which has a *para* arrangement of CN and Ph groups). The overall average predicted change in $E_{1/2}$ is +0.10 V upon adding a phenyl group relative to the experimental $E_{1/2}$ values of the parent cyanopyridine (see Table 1). The computations thus reinforce our hypothesis that phenyl-substituted derivatives should maintain the low $E_{1/2}$ desirable in an RFB anolyte.

Of the three cyanopyridine isomers, dimerization of the radical anion is most favorable for 3-CNPy$^{\bullet-}$. To examine whether adding a phenyl group is likely to prevent dimerization, the electronic structures of the radical anion of the four isomers of 3-cyano-x-phenylpyridine were calculated (B3LYP/6-311+G**//B3LYP/6-31G*, "polar solvent"). Figure 5 is a visualization of the isosurfaces of the calculated Mulliken spin density for the four 3-CN-x-PhPy$^{\bullet-}$ radical anions (the values of the spin density are given in Figure S2). The amount of spin density delocalized onto the phenyl ring depends strongly on its position on the pyridine ring. In 3-CN-5-PhPy$^{\bullet-}$, where the phenyl group is *meta* to the cyano group, there is almost no spin density on the phenyl ring, as can be seen in Figure 5. In contrast, when the phenyl group is either *para* or *ortho* to the cyano group, which is the case for all three of the other isomers, there is significant spin delocalization on the phenyl ring. In each of those three isomers, the greatest amount of spin density on the phenyl ring is at its 4-position, although the values of spin density at that position (0.182, 0.175, and 0.164 for 3-CN-6-PhPy$^{\bullet-}$, 3-CN-4-PhPy$^{\bullet}$, and 3-CN-2-PhPy$^{\bullet-}$, respectively) indicate that it is unlikely that dimerization would occur at that site (compared to the spin density of 0.326 at the 5-position of 2-CNPy$^{\bullet-}$ (Figure 4), a radical anion for which only a

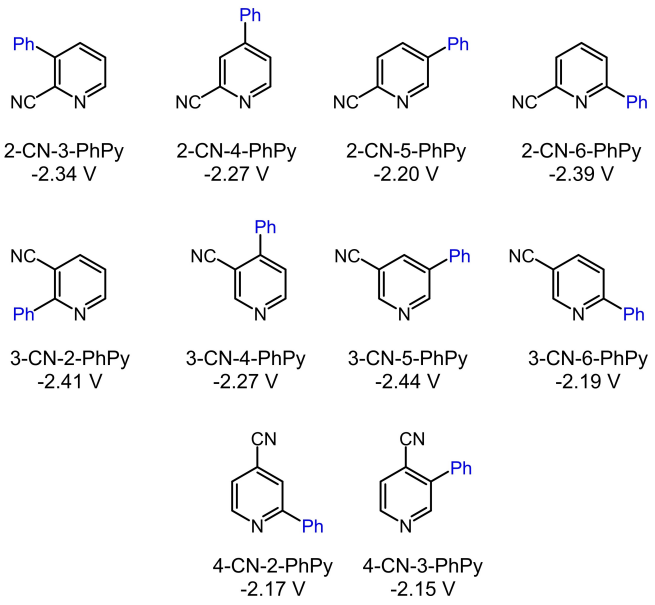

Figure 4. Structures of the cyanophenylpyridines and their computationally predicted reduction potentials.

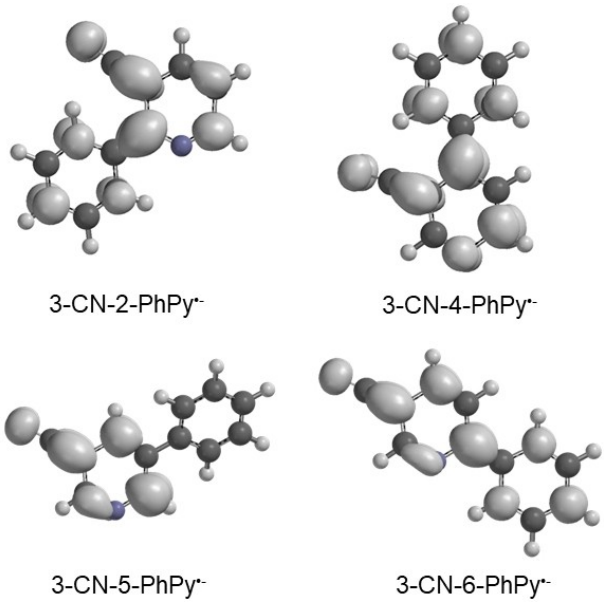

Figure 5. Mulliken spin density isosurfaces for 3-CN-2-PhPy$^{\bullet-}$, 3-CN-4-PhPy$^{\bullet-}$, 3-CN-5-PhPy$^{\bullet-}$ and 3-CN-6-PhPy$^{\bullet-}$ radical anions.

very small amount of dimerization was observed in the CV). Dimerization is more likely to occur at a carbon of the pyridine ring, where higher spin densities are present. Specifically, the 6-carbon of 3-CN-5-PhPy$^{\bullet-}$ has a high calculated spin density of 0.474, indicating that dimerization is likely. For the three other isomers, the largest spin density on the pyridine ring occurs at the carbon where the phenyl ring is bonded, which likely provides some steric protection against dimerization.

The ΔG_{dim} was calculated for the four 3-CN-x-PhPy$^{\bullet-}$ isomers by the same method used for the cyanopyridine radical anions: geometry-optimization and vibrational analysis in the gas phase (B3LYP-D3/6-311++G**) and then a single-point energy calculation in solvent (B3LYP-D3/6-311++G**) for a solvation energy correction. For each radical anion, the most likely sites for dimerization are the pyridine carbon atoms with the highest calculated spin densities (Figure 5 and S2) and no sterically blocking phenyl or cyano group, so the dimerization free energies were calculated for those sites. The results are shown in Table 3, with further details in Table S3. For 3-CN-5-PhPy$^{\bullet-}$ the calculated ΔG_{dim} (-11.6 kcal/mol at the more favored C-4 position) is more negative than that of the parent 3-CNPy$^{\bullet-}$, suggesting that 3-CN-5-PhPy$^{\bullet-}$ is very likely to dimerize. The radical anion 3-CN-2-PhPy$^{\bullet-}$ also has a negative calculated ΔG_{dim}, −1.2 kcal/mol, for dimerization at C-6. For 3-CN-4-PhPy$^{\bullet-}$ $\Delta G_{dim} = +3.1$ kcal/mol, while for 3-CN-6-PhPy$^{\bullet-}$ $\Delta G_{dim} = +6.7$ kcal/mol (at C-4), which indicates that 3-CN-6-PhPy and 3-CN-4-PhPy are the least likely to dimerize and are therefore the most promising anolytes from this group.

Table 3. Calculated free energies of dimerization of cyanophenylpyridine radical anions.

radical anion	site of dimerization	solution-phase dimerization ΔG [kcal/mol]
3-CN-2-PhPy$^{\bullet-}$	C6	−1.2
3-CN-4-PhPy$^{\bullet-}$	C6	3.1
3-CN-5-PhPy$^{\bullet-}$	C4	−11.6
3-CN-5-PhPy$^{\bullet-}$	C6	−6.0
3-CN-6-PhPy$^{\bullet-}$	C4	6.7
3-CN-6-PhPy$^{\bullet-}$	C6	23.3

Table 4. Experimental and calculated reduction potentials of cyanophenylpyridines.

molecule	experimental $E_{1/2}$ (V vs. $Fc^{+/0}$)	calculated $E_{1/2}$ (V vs. $Fc^{+/0}$)
2-CN-3-PhPy	−2.35	−2.34
2-CN-4-PhPy	−2.22	−2.27
2-CN-5-PhPy	−2.24	−2.20
2-CN-6-PhPy	−2.36	−2.39
3-CN-2-PhPy	−2.36 ($E_{p/2}$)	−2.41
3-CN-4-PhPy	−2.22	−2.27
3-CN-5-PhPy	−2.29 ($E_{p/2}$)	−2.44
3-CN-6-PhPy	−2.19	−2.19
4-CN-2-PhPy	−2.19	−2.17
4-CN-3-PhPy	−2.13	−2.15

Synthesis and Electrochemical Characterization of the Ten Cyanophenylpyridine Isomers

All ten cyanophenylpyridine isomers were synthesized by Suzuki-Miyaura coupling of an appropriate halocyanopyridine and phenylboronic acid. For example, 2-CN-3-PhPy was synthesized by the palladium-catalyzed reaction of 3-bromo-2-cyanopyridine with phenylboronic acid in dimethoxyethane/K_2CO_3 (*aq*), as shown in Scheme 2. The other isomers were synthesized similarly from the appropriate bromocyanopyridine or chlorocyanopyridine and were purified by flash chromatography. Synthetic details are given in the Supporting Information. All of these molecules, like the parent cyanopyridines, are stable to air, water, and light, but when reduced to their radical anions, they are oxygen and water sensitive.

Cyclic voltammetry on each cyanophenylpyridine isomer was conducted in CH_3CN containing 0.50 M $[NBu_4][PF_6]$ under the same experimental conditions described for the parent cyanopyridines. Two example CVs are shown in Figure 6, for 3-CN-5-PhPy (irreversible reduction) and 3-CN-6-PhPy (reversible reduction), and the remaining CVs are in the Supporting Information. For most of the isomers, the reduction was reversible or there was only a very small peak due to dimeric dianion re-oxidation evident in the CV. For 3-CN-5-PhPy and 3-CN-2-PhPy the reduction was irreversible (and nearly all re-oxidations occurred through the dimeric dianion), in accord with the DFT predictions. The $E_{1/2}$ (or $E_{p/2}$) for each cyanophenylpyridine isomer is given in Table 4, along with the previously calculated values. There is good agreement with the calculated $E_{1/2}$ values, with an average deviation from the predictions of only 28 mV. The largest deviation is 150 mV for 3-CN-5-PhPy, and that is for an $E_{p/2}$ value, which is only an estimate of $E_{1/2}$ due to the irreversibility. The average reduction potential of all ten isomers is −2.255 V, which, as predicted, represents a small shift (+98 mV) relative to the average reduction potential of the three cyanopyridine isomers.

While all of the electrochemical experiments to this point were conducted in CH_3CN with 0.50 M $[NBu_4][PF_6]$, the cyclic voltammetry of 3-CN-6-PhPy was further examined in CH_3CN with 0.50 M KPF_6 to determine the effect of a different supporting electrolyte cation on dimerization. Because K^+ can

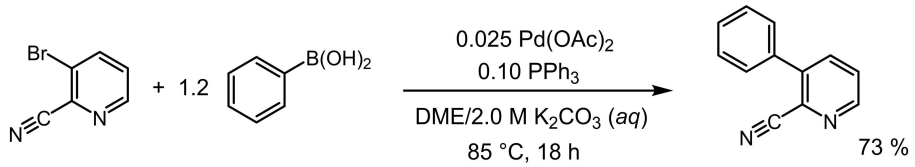

Scheme 2. Synthesis of 2-cyano-3-phenylpyridine.

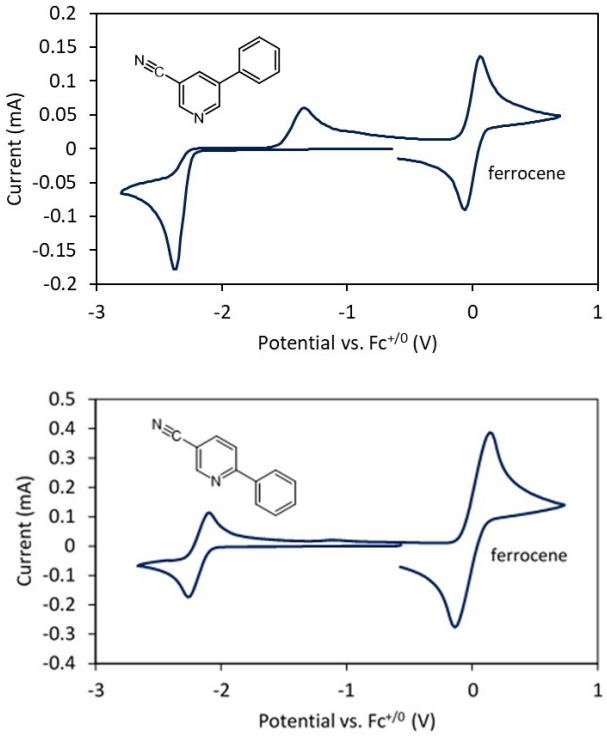

Figure 6. Cyclic voltammograms of 10 mM 3-CN-5-PhPy (top) and 3-CN-6-PhPy (bottom) at a glassy carbon electrode in CH_3CN with 0.50 M $[NBu_4][PF_6]$ at a scan rate of 100 mV/s, both with a ferrocene internal standard. Dimerization of the radical anion of 3-CN-5-PhPy results in re-oxidation (of the dimer) at a positively shifted potential.

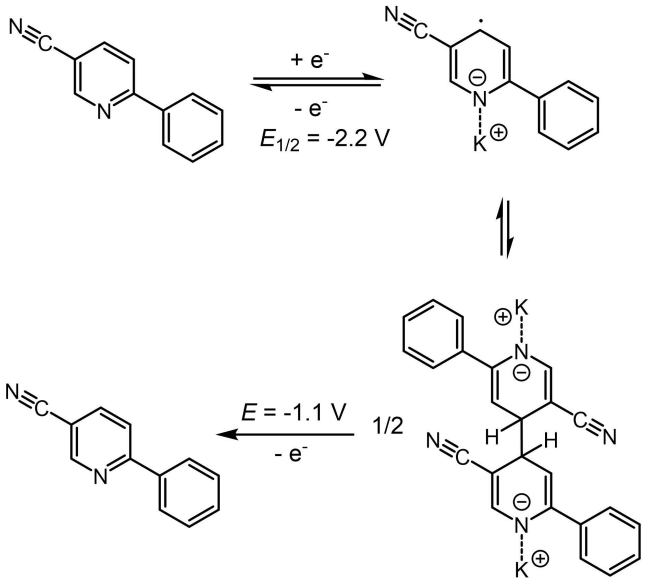

Scheme 3. Reduction of 3-CN-6-PhPy in the presence of K^+ followed by reversible dimerization of K^+ 3-CN-6-PhPy$^{\bullet-}$ to $(K^+$ 3-CN-6-PhPy$^{\bullet-})_2$ and irreversible oxidation of $(K^+$ 3-CN-6-PhPy$^{\bullet-})_2$.

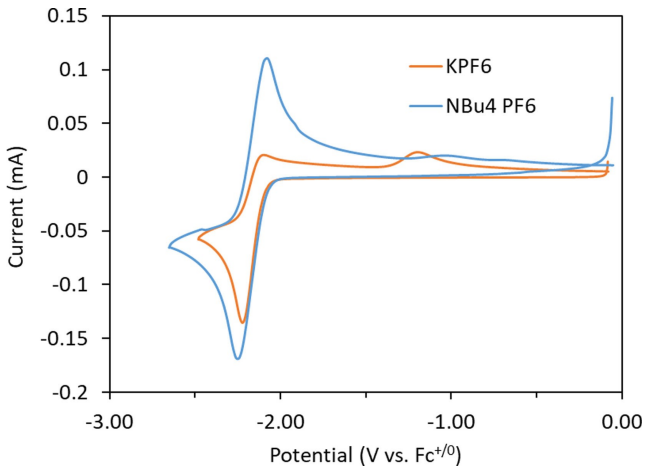

Figure 7. Cyclic voltammograms of 10 mM 3-CN-6-PhPy at a glassy carbon electrode in CH_3CN with 0.50 M $[NBu_4][PF_6]$ and with 0.50 M KPF_6 at a scan rate of 100 mV/s.

form a tight ion pair with the 3-CN-6-PhPy$^{\bullet-}$ radical anion, particularly through the direct coordination of the pyridine nitrogen lone pair to K^+, it was expected to decrease the coulombic repulsion of the radical anions and make dimerization more favorable. The proposed reduction followed by dimerization equilibrium is shown in Scheme 3, with dimerization occurring at C-4, the site predicted by DFT calculations (see Table 3). Figure 7 shows the CVs of 3-CN-6-PhPy in CH_3CN with 0.50 M KPF_6 and with 0.50 M $[NBu_4][PF_6]$ supporting electrolyte and otherwise identical conditions, except for a slightly higher concentration of 3-CN-6-PhPy in the KPF_6 experiment (scan rate = 100 mV/s). The CV in 0.50 M $[NBu_4][PF_6]$ shows a reduction of 3-CN-6-PhPy to the radical anion at ca. −2.2 V and then a re-oxidation with $i_{pa} \approx i_{pc}$. There is a very small oxidative peak at ca. −1.1 V due to oxidation of dimeric dianion. In contrast, the CV in 0.50 M KPF_6 has a significantly decreased i_{pa} for radical anion oxidation, replaced by a significant dimeric dianion re-oxidation at ca. −1.1 V. Thus, the hypothesis that K^+ would lead to more dimerization than NBu_4^+ is supported, and a change in the supporting electrolyte provides a straightforward means to tune the amount of dimerization that occurs in these anolytes.

Varying the scan rate of a CV will change its appearance significantly if a reversible dimerization is occurring, and the 3-CN-6-PhPy CV with KPF_6 supporting electrolyte provides a useful test case where it appears that the K^+ 3-CN-6-PhPy$^{\bullet-}$ dimerization equilibrium constant is not far from 1. Therefore, the CVs of 3-CN-6-PhPy in CH_3CN with 0.50 M KPF_6 were collected at 10, 100, and 250 mV/s, as shown in Figure 8. At the fastest scan rate of 250 mV/s, the radical anion is formed in the negative sweep and then partially dimerizes. In the positive sweep some radical anion is re-oxidized near the $E_{1/2}$ of −2.2 V, and then at potentials between −2.2 V and −1.1 V (where the potential is positive enough to oxidize the radical anion but not the dimeric dianion), there is some further oxidation as dimer dissociates to radical anion, which is oxidized to neutral 3-CN-6-PhPy. However, at this fast scan rate there is dimer remaining at −1.1 V to be oxidized, as evidenced by the peak near −1.1 V in the CV. In contrast, at the slowest scan rate of 10 mV/s the same reduction to radical anion and partial dimerization occurs,

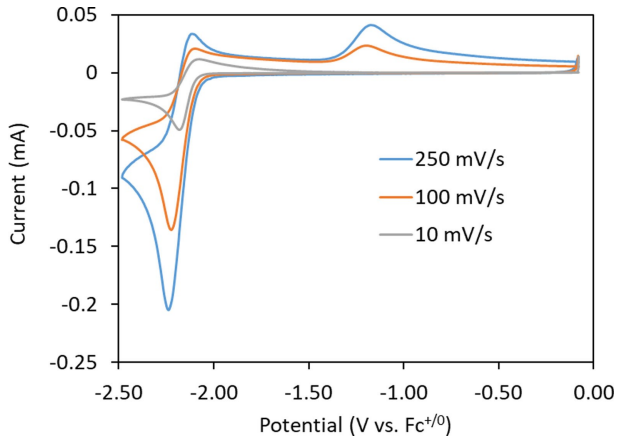

Figure 8. Cyclic voltammograms of 10 mM 3-cyano-6-phenylpyridine at a glassy carbon electrode in CH_3CN with 0.50 M KPF_6 at scan rates of 10, 100, and 250 mV/s.

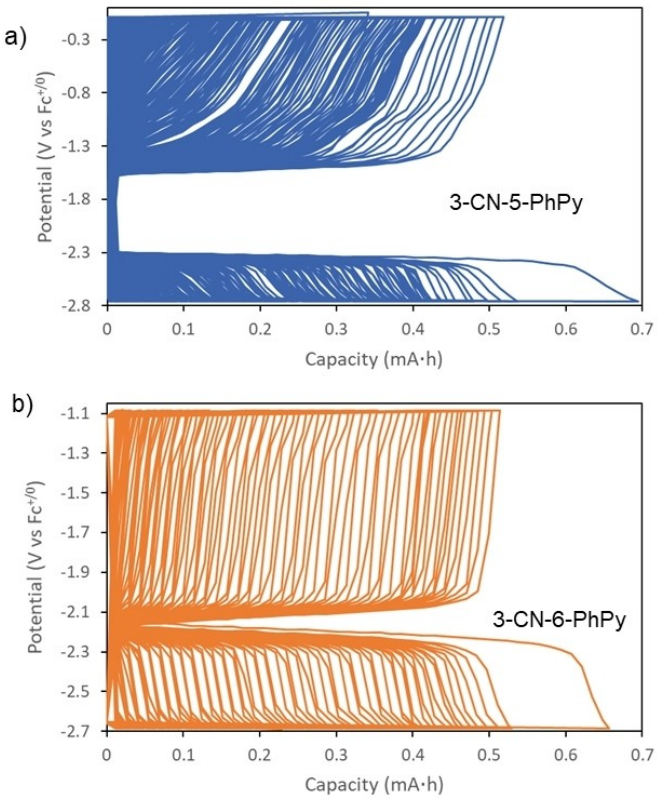

Figure 9. Charge-discharge curves (5.0 mL of a 5.0 mM solution of active material in 0.50 M $[NBu_4][PF_6]$ in CH_3CN; current = 5.00 mA) for (a) 3-CN-5-PhPy and (b) 3-CN-6-PhPy. Theoretical capacity is 0.67 mAh.

but the slow positive sweep allows all the dimers to dissociate to radical anion (the vertical equilibrium in Scheme 3) as the radical anion is consumed through re-oxidation to the neutral molecule at potentials between −2.2 and −1.1 V. There is therefore no dimeric dianion remaining when the sweep reaches −1.1 V and there is no oxidation peak at −1.1 V in the 10 mV/s CV. All these observations are consistent with the proposed reversible dimerization of K^+ 3-CN-6-PhPy$^{\bullet-}$.

The most favorable conditions for dimerization of a radical anion would be with the 3-CN-5-PhPy isomer in CH_3CN with KPF_6 supporting electrolyte. To spectroscopically observe this dimer, 3-CN-5-PhPy was reductively bulk electrolyzed in CD_3CN/KPF_6 and the ^1H NMR spectrum of the resulting orange solution was collected (Figure S5), but it was too complex for definitive interpretation.

To examine their behavior during charge-discharge cycling, all ten cyanophenylpyridine isomers were subjected to bulk charge-discharge cycling in an H-cell in CH_3CN with 0.50 M $[NBu_4][PF_6]$ supporting electrolyte and other conditions identical to those for the cyanopyridines. Example sets of charge-discharge curves for 3-CN-5-PhPy and 3-CN-6-PhPy are shown in Figure 9. The molecule 3-CN-6-PhPy charges and discharges near −2.2 V, its reversible $E_{1/2}$ determined by cyclic voltammetry. In contrast, 3-CN-5-PhPy charges at −2.3 V (its irreversible $E_{p/2}$) and then discharges through the dimer at approximately −1.5 V. Thus 3-CN-5-PhPy would lose about 0.8 V between charge and discharge in an RFB and is not a good candidate for an RFB anolyte.

Another important consideration for RFB anolytes is capacity retention during cycling. Figure 10 shows the discharge capacity versus cycle number for several bulk charge-discharge cycling experiments for 3-CN-5-PhPy and 3-CN-6-PhPy (others are given in the Supporting Information). After an initial drop in capacity, both retain capacity reasonably well: after the initial two cycles, 3-CN-5-PhPy loses on average 0.65% capacity per cycle through cycle 30 (4.8–5.5 h), while 3-CN-6-PhPy loses on average 1.2% capacity per cycle through the same span. In fact, 3-CN-5-PhPy shows the best capacity retention of the ten isomers examined, but that is likely due to the fact that it exists in solution almost exclusively as the dimeric dianion and not as a free radical, which are known to undergo decomposition reactions such as hydrogen atom abstraction from solvent. Moreover, the 3-CN-5-PhPy dimeric dianion has a significantly more positive reduction potential than the monomeric radical anions, which likely makes it less basic and therefore less prone to proton abstraction from solvent or electrolyte. Also shown in Figure 10 is the Coulombic efficiency for one representative experiment for each molecule. For 3-CN-5-PhPy the Coulombic efficiency drops over the first several cycles and then is steady at about 96%, while for 3-CN-6-PhPy the Coulombic efficiency drops over the first several cycles and then is (fairly) steady at 97–98%. Figure 11 shows the capacity retention of the ten cyanophenylpyridines through 30 cycles (including the first cycle). The data shows that the 3-CN-x-PhPy isomers are the most stable during charge-discharge cycling. However, both 3-CN-5-PhPy$^{\bullet-}$ and 3-CN-2-PhPy$^{\bullet-}$ dimerize, which will lead to a significant decrease in voltaic efficiency in an RFB. Taking all this data into consideration, among the cyanophenylpyridines, 3-CN-6-PhPy and 3-CN-4-PhPy are the most promising anolytes for nonaqueous RFBs, both with a low reduction potential of approximately −2.2 V vs. $Fc^{+/0}$ and good stability during cycling.

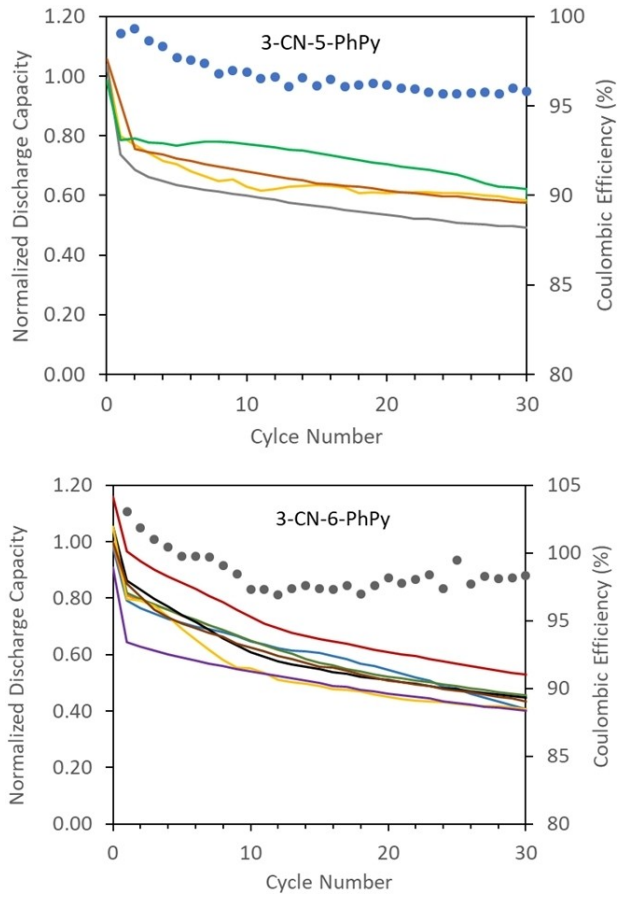

Figure 10. Normalized discharge capacity (solid lines) versus cycle number during bulk charge-discharge cycling for four runs for 3-CN-5-PhPy (top) and six runs for 3-CN-6-PhPy (bottom). All runs used 5.0 mL of a 5.0 mM solution of active material in 0.50 M $[NBu_4][PF_6]$ in CH_3CN, with a current of 5.00 mA. Capacity (left axis) is normalized to a theoretical capacity of 0.67 mAh. Coulombic efficiency (right axis) is shown as individual points for one representative run.

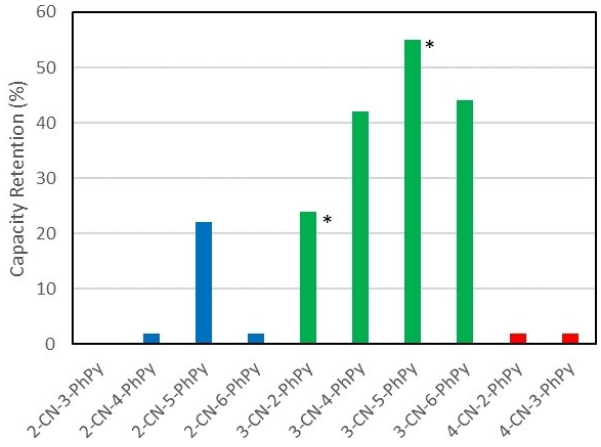

Figure 11. Capacity retention of cyanophenylpyridines through 30 cycles of charge-discharge cycling. An asterisk indicates dimerization of the radical anion during cycling.

3-Cyano-4-methyl-6-(3,5-dimethylphenyl)pyridine

To further improve the stability of the cyanophenylpyridine anolytes, some methylated versions were evaluated. Methyl groups add steric blocking that will inhibit H-atom abstraction from solvent or electrolyte (one likely decomposition route), while their electron-donating character will shift $E_{1/2}$ in the desirable negative direction. Particularly promising was 3-cyano-4-methyl-6-(3,5-dimethylphenyl)pyridine (Me_3-3-CN-6-PhPy), shown in Figure 12. It has a predicted $E_{1/2}$ of −2.29 V vs. ferrocene, which is 0.10 V more negative than its parent 3-CN-6-PhPy. Cyclic voltammetry of Me_3-3-CN-6-PhPy in CH_3CN with 0.50 M $[NBu_4][PF_6]$ (see Supporting Information) showed that it had an $E_{1/2}$ of −2.50 V vs. $Fc^{+/0}$.

To test the stability of Me_3-3-CN-6-PhPy under cycling conditions, it was subjected to bulk charge-discharge cycling under conditions identical to the cyanopyridines. Figure 13 shows the capacity versus cycle number for four separate runs of charge-discharge cycling. After the initial few cycles, capacity loss is quite steady and consistent between experiments, at 0.21% per cycle. That is about one-sixth the capacity fade rate of 1.2% per cycle for 3-CN-6-PhPy, showing a significant improvement in stability with addition of the methyl groups.

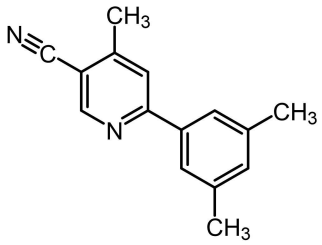

Figure 12. Structure of 3-cyano-4-methyl-6-(3,5-dimethylphenyl)pyridine (Me_3-3-CN-6-PhPy).

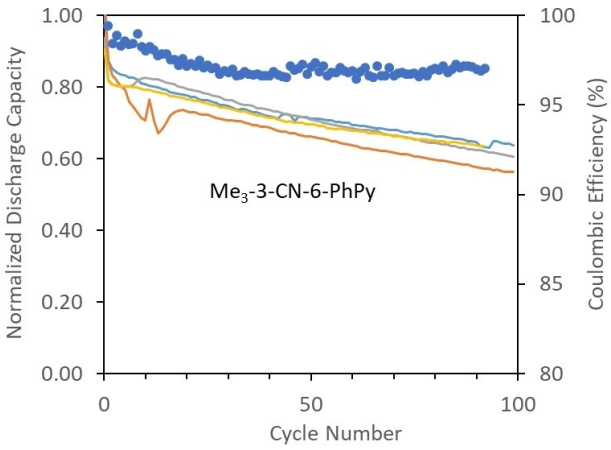

Figure 13. Normalized discharge capacity (solid lines) versus cycle number for four runs of bulk charge-discharge cycling of Me_3-3-CN-6-PhPy. All runs used 5.0 mL of a 5.0 mM solution of active material in 0.50 M $[NBu_4][PF_6]$ in CH_3CN, with a current of 5.00 mA. Capacity (left axis) is normalized to a theoretical capacity of 0.67 mAh. Coulombic efficiency (right axis) is shown as individual points for one representative run.

Coulombic efficiency, also shown in Figure 13, was steady at about 97% after the initial drop.

The solubility of redox-active molecules is an important parameter for RFBs, as it partly determines the energy density of an RFB. We determined that Me_3-3-CN-6-PhPy has a solubility of 0.19 M in our electrolyte system of 0.50 M $[NBu_4][PF_6]$ in CH_3CN. For comparison, we determined the solubility of the parent 3-CN-6-PhPy in the same electrolyte system and found that it is, surprisingly, significantly higher at 0.71 M. If desired, it is likely that the solubility of the 3-CN-6-PhPy molecular core could be increased significantly, while maintaining the stability of Me_3-3-CN-6-PhPy, by functionalization with short ethylene glycol chains in place of the methyl groups.[24]

Overall Me_3-3-CN-6-PhPy is a highly optimized nonaqueous RFB anolyte. Its most striking characteristic is its extremely low reduction potential of −2.50 V vs. $Fc^{+/0}$, while maintaining good cycling stability in acetonitrile. Other reported nonaqueous RFB anolytes with low reduction potentials include 2-methylbenzophenone with $E_{1/2} = -2.34$ V vs. $Fc^{+/0}$,[19] *N*-methylphthalimide[25] (−1.97 V vs. $Fc^{+/0}$), 9-fluorenone[26] (-1.84 V vs. $Fc^{+/0}$), and 2,1,3-benzothiadiazole[27] (−1.78 V vs. $Fc^{+/0}$), but we have found no reports of an anolyte with a lower reduction potential than Me_3-3-CN-6-PhPy. (It is not possible to directly compare the capacity retention of Me_3-3-CN-6-PhPy and these other low-potential anolytes because the latter were studied as full RFBs with different catholytes. Table S4 lists some data from those RFBs, including capacity fade rates.)

Conclusions

The previously reported reversible reduction of cyanopyridines indicated that they might serve as good anolytes for nonaqueous RFBs. However, 3-CNPy shows a strong tendency to dimerize when reduced to $3\text{-CNPy}^{\bullet-}$, which leads to a large potential change between reduction and oxidation. In addition, 2-CNPy and 4-CNPy have low stability during bulk charge-discharge cycling, rendering them unsuitable as RFB anolytes. DFT calculations predicted that adding a phenyl group to the cyanopyridines would, for some isomers, increase stability of the radical anions by delocalizing the negative charge and unpaired spin density and would also make dimerization less favorable, all while causing only a small positive shift in reduction potential. All ten isomers of cyanophenylpyridine were synthesized and studied by CV and bulk charge-discharge cycling. Among these, the 3-CN-x-PhPy isomers showed the greatest stability during charge-discharge cycling. However, both $3\text{-CN-2-PhPy}^{\bullet-}$ and $3\text{-CN-5-PhPy}^{\bullet-}$ radical anions dimerize, which would result in low voltaic efficiency in an RFB. Of the cyanophenylpyridines, the isomers 3-CN-6-PhPy and 3-CN-4-PhPy are the most promising anolytes, both with a low reduction potential of approximately −2.2 V vs. $Fc^{+/0}$ and reasonable stability during cycling. An improved version of 3-CN-6-PhPy, Me_3-3-CN-6-PhPy, has an extremely low reduction potential of −2.50 V vs. $Fc^{+/0}$ (the lowest among reported nonaqueous RFB anolytes) and loses only 0.21% of capacity per cycle during charge-discharge cycling in acetonitrile.

Experimental Section

Synthetic Procedures

General Information: All commercial chemicals were used as received unless stated otherwise. Cyanopyridines and 2-CN-4-PhPy were purchased, while the other cyanophenylpyridines and 3-cyano-4-methyl-6-(3,5-dimethylphenyl)pyridine (Me_3-3-CN-6-PhPy) were synthesized as described below. NMR spectra were obtained on Varian V NMRS 700, Varian V NMRS 500, Varian Inova 500, or Varian MR400 spectrometers. ^1H and ^{13}C chemical shifts are reported in parts per million (ppm) relative to residual $CHCl_3$ at 7.26 ppm (^1H) or $CDCl_3$ at 77.16 ppm (^{13}C).

2-CN-3-PhPy. General procedure for cyanophenylpyridine synthesis: A 50 mL round bottom flask was charged with 3-bromo-3-cyanopyridine (1.067 g, 5.83 mmol), phenylboronic acid (880 mg, 7.22 mmol), triphenylphosphine (156 mg, 0.595 mmol), and a magnetic stir bar. The flask was fitted with a condenser and rubber septum and flushed with nitrogen. A portion of K_2CO_3 (2.77 g, 20 mmol) was diluted in water to 10 mL to create a 2.0 M solution, which was sparged with N_2 for 30 minutes. The K_2CO_3 (*aq*) solution was added to the reaction mixture. In a nitrogen-filled glovebox, $Pd(OAc)_2$ (35 mg, 0.16 mmol) was dissolved in 10 mL 1,2-dimethoxyethane. The $Pd(OAc)_2$ solution was removed from the glovebox and added by a syringe to the reaction mixture. The reaction was stirred at reflux under N_2 for 18 h. The resulting reaction mixture was extracted with ethyl acetate and water and the organic extracts dried over $MgSO_4$. After evaporation of the solvent the product was purified by flash chromatography on silica (17% ethyl acetate in hexanes). Yield 768 mg (73%). m.p. 88–90 °C. ^1H NMR (500 MHz, $CDCl_3$) δ 8.70 (dd, J = 4.7, 1.6 Hz, 1H), 7.87 (dd, J = 8.0, 1.6 Hz, 1H), 7.60–7.55 (m, 3H), 7.55–7.50 (m, 3H). ^{13}C NMR (126 MHz, $CDCl_3$) δ 149.55, 142.25, 137.76, 135.43, 132.34, 129.62, 129.20, 128.89, 126.75, 117.10.

2-CN-4-PhPy: Purchased. ^1H NMR (500 MHz, $CDCl_3$) δ 8.75 (dd, J = 5.2, 1.7 Hz, 1H), 7.91 (s, 1H), 7.71 (dd, J = 5.0, 2.4 Hz, 1H), 7.66–7.60 (m, 2H), 7.57–7.49 (m, 3H). ^{13}C NMR (126 MHz, $CDCl_3$) δ 151.61, 149.96, 136.08, 134.69, 130.34, 129.65, 127.12, 126.59, 124.71, 117.48.

2-CN-5-PhPy: The general procedure was followed with 5-chloro-2-cyanopyridine as the halocyanopyridine reactant. Yield: 61%. m.p. 68–69 °C. ^1H NMR (500 MHz, $CDCl_3$) δ 8.95 (d, J = 2.1 Hz, 1H), 8.01 (dd, J = 8.0, 2.3 Hz, 1H), 7.77 (dd, J = 8.1, 0.9 Hz, 1H), 7.63-7.57 (m, 2H), 7.57-7.46 (m, 3H). ^{13}C NMR (126 MHz, $CDCl_3$) δ 149.78, 140.01, 136.03, 135.02, 132.41, 129.61, 129.59, 128.58, 127.47, 117.48.

2-CN-6-PhP: The general procedure was followed with 6-bromo-2-cyanopyridine as the halocyanopyridine reactant. Yield: 83%. m.p. 64–65 °C. ^1H NMR (500 MHz, $CDCl_3$) δ 8.03 (dd, J = 7.8, 1.8 Hz, 2H), 7.95 (d, *J* = 8.1 Hz, 1H), 7.89 (t, *J* = 7.8 Hz, 1H), 7.62 (d, *J* = 7.5 Hz, 1H), 7.53–7.46 (m, 3H). ^{13}C NMR (126 MHz, $CDCl_3$) δ 159.12, 137.85, 137.33, 133.98, 130.33, 129.14, 127.20, 126.73, 123.61, 117.56.

3-CN-2-PhPy: The general procedure was followed with 2-chloro-3-cyanopyridine as the halocyanopyridine reactant. Yield: 80%. m.p. 70–72 °C. ^1H NMR (500 MHz, $CDCl_3$) δ 8.89 (dd, J = 4.8, 1.9 Hz, 1H), 8.08 (dd, J = 7.9, 1.8 Hz, 1H), 7.93 (m, 2H), 7.53 (m, 3H), 7.38 (dd, J = 7.7, 5.1 Hz, 1H). ^{13}C NMR (126 MHz, $CDCl_3$) δ 161.11, 152.74, 141.91, 137.25, 130.33, 128.97, 128.79, 121.64, 117.74, 107.58.

3-CN-4-PhPy: The general procedure was followed with 4-chloro-3-cyanopyridine as the halocyanopyridine reactant. Yield: 16%. ^1H NMR (500 MHz, $CDCl_3$) δ 8.96 (s, 1H), 8.81 (d, J = 5.2 Hz, 1H), 7.66–7.59 (m, 2H), 7.59–7.50 (m, 3H), 7.48 (d, J = 5.2 Hz, 1H). ^{13}C NMR (126 MHz, $CDCl_3$) δ 154.17, 152.96, 152.46, 135.54, 130.39, 129.33, 128.52, 123.89, 116.83, 108.72.

3-CN-5-PhPy: The general procedure was followed with 5-bromo-3-cyanopyridine as the halocyanopyridine reactant. Yield: 45%. ^{1}H NMR (500 MHz, $CDCl_3$) δ 9.03 (d, J = 2.3 Hz, 1H), 8.85 (d, J = 2.0 Hz, 1H), 8.13 (t, J = 2.1 Hz, 1H), 7.59–7.51 (m, 4H), 7.50–7.46 (m, 1H). ^{13}C NMR (126 MHz, $CDCl_3$) δ 151.66, 150.82, 137.35, 137.13, 135.58, 129.62, 129.40, 127.31, 116.71, 110.24.

3-CN-6-PhPy: The general procedure was followed with 6-chloro-3-cyanopyridine as the halocyanopyridine reactant. Flash chromatography used 12% ethyl acetate in hexanes. Yield: 78%. m.p. 67–68 °C. ^{1}H NMR (500 MHz, $CDCl_3$) δ 8.95 (d, *J* = 2.2 Hz, 1H), 8.05 (dd, *J* = 7.6, 2.1 Hz, 2H), 8.01 (dd, *J* = 8.3, 2.2 Hz, 1H), 7.86 (d, *J* = 8.3 Hz, 1H), 7.55-7.48 (m, 3H). ^{13}C NMR (126 MHz, $CDCl_3$) δ 160.67, 152.61, 140.01, 137.51, 130.77, 129.23, 127.52, 120.14, 117.14, 108.02.

4-CN-2-PhPy: The general procedure was followed with 2-chloro-4-cyanopyridine as the halocyanopyridine reactant. Yield: 94%. m.p. 54–55 °C. ^{1}H NMR (500 MHz, $CDCl_3$) δ 8.86 (dd, J = 5.0, 0.9 Hz, 1H), 8.02–7.98 (m, 2H), 7.94 (t, J = 1.3 Hz, 1H), 7.54–7.47 (m, 3H), 7.44 (dd, J = 4.9, 1.5 Hz, 1H). ^{13}C NMR (126 MHz, $CDCl_3$) δ 158.88, 150.76, 137.44, 130.35, 129.22, 127.10, 123.29, 122.17, 121.33, 116.87.

4-CN-3-PhPy: The general procedure was followed with 3-bromo-4-cyanopyridine as the halocyanopyridine reactant. Yield: 87%. m.p. 80 °C. ^{1}H NMR (500 MHz, $CDCl_3$) δ 8.87 (s, 1H), 8.75 (d, J = 5.0 Hz, 1H), 7.62 (d, J = 5.0 Hz, 1H), 7.61–7.58 (m, 2H), 7.57–7.48 (m, 3H). ^{13}C NMR (126 MHz, $CDCl_3$) δ 151.13, 148.86, 138.83, 134.55, 129.69, 129.28, 128.93, 126.17, 118.95, 116.46.

Me_3-3-CN-6-PhPy: The general procedure was followed with 3-cyano-4-methyl-6-bromopyridine as the halocyanopyridine reactant and 3,5-dimethylphenylboronic acid as the aryl reactant. Yield: 60%. ^{1}H NMR (500 MHz, $CDCl_3$) δ 8.82 (s, 1H), 7.67 (s, 1H), 7.63 (s, 2H), 7.12 (s, 1H), 2.60 (s, 3H), 2.40 (s, 6H). ^{13}C NMR (126 MHz, $CDCl_3$) δ 160.64, 152.69, 151.24, 138.76, 137.59, 132.24, 125.32, 121.40, 116.60, 108.76, 21.50, 20.54.

Electrochemical Methods

Materials: Acetonitrile (anhydrous, 99.8%) was obtained from Sigma Aldrich. Tetrabutylammonium hexafluorophosphate ($[NBu_4][PF_6]$; electrochemical grade) was obtained from Sigma Aldrich and transferred to a N_2-filled glovebox. Potassium hexafluorophosphate (KPF_6; electrochemical grade) was obtained from Sigma Aldrich and dried under high vacuum for 48 h at 70 °C before being transferred to a N_2-filled glovebox. Stock solutions (0.50 M) of $[NBu_4][PF_6]$ and KPF_6 in acetonitrile was prepared in a N_2-filled glovebox and stored over 3 Å molecular sieves for at least two days prior to use.

Cyclic voltammetry: Cyclic voltammetry (CV) was performed in a N_2-filled glovebox with a Biologic VSP multichannel potentiostat/galvanostat using a three-electrode electrochemical cell, consisting of a glassy carbon disk working electrode (0.071 cm^2, BASi), a Ag/Ag^+ reference electrode (BASi) with 0.01 M $AgBF_4$ (Sigma) and 0.50 M $[NBu_4][PF_6]$ in acetonitrile, and a platinum wire counter electrode. Potentials were referenced to an internal standard of ferrocene. Experiments were conducted on a 10 mM solution of analyte in a 0.50 M $[NBu_4][PF_6]$ solution in acetonitrile at scan rates of 100 mV/s unless noted otherwise.

Bulk charge-discharge cycling: Bulk charge/discharge measurements were carried out in a N_2-filled glovebox with a BioLogic VSP galvanostat in a custom glass H-cell with an ultrafine fritted glass separator (P5, Adams and Chittenden). The working and counter electrodes were reticulated vitreous carbon (100 ppi, ~70 cm^2 surface area, Duocel). A Ag/Ag^+ reference electrode was used on the working side of the H-cell. The electrolyte solution contained 5 mM active species and 0.50 M $[NBu_4][PF_6]$ in acetonitrile. The working chamber and counter chamber of the H-cell were both loaded with 5.0 mL of the electrolyte + active species solution. Both chambers were stirred continuously during cycling at a current of 5 mA. Voltage cutoffs of approximately 0.5 V lower than $E_{1/2}$ and 1.0 V higher than $E_{1/2}$ were used for charging and discharging, respectively. After one charging cycle (no discharge), the counter electrode chamber was emptied and replaced with a fresh 5.0 mL of electrolyte + active species solution, along with a new RVC electrode. After that first half-cycle, charge-discharge cycles were resumed.

Acknowledgements

This work was supported as part of the Joint Center for Energy Storage Research (JCESR), an Energy Innovation Hub funded by the U.S. Department of Energy, Office of Science, Basic Energy Sciences.

Conflict of Interest

The authors declare no conflict of interest.

Data Availability Statement

The data that support the findings of this study are available from the corresponding author upon reasonable request.

Keywords: cyanopyridines · reduction potential · redox-flow battery · reduction potential calculation · reversible dimerization

[1] G. L. Soloveichik, *Chem. Rev.* **2015**, *115*, 11533–11558.
[2] J. Winsberg, T. Hagemann, T. Janoschka, M. D. Hager, U. S. Schubert, *Angew. Chem. Int. Ed.* **2017**, *56*, 686–711; *Angew. Chem.* **2017**, *129*, 702–729.
[3] J. Noack, N. Roznyatovskaya, T. Herr, P. Fischer, *Angew. Chem. Int. Ed.* **2015**, *54*, 9776–9809; *Angew. Chem.* **2015**, *127*, 9912–9947.
[4] R. F. Service, *Science* **2018**, *362*, 508.
[5] P. Leung, A. A. Shah, L. Sanz, C. Flox, J. R. Morante, Q. Xu, M. R. Mohamed, C. Ponce de León, F. C. Walsh, *J. Power Sources* **2017**, *360*, 243–283.
[6] J. A. Kowalski, L. Su, J. D. Milshtein, F. R. Brushett, *Curr. Opin. Chem. Eng.* **2016**, *13*, 45–52.
[7] Y. Yan, S. G. Robinson, M. S. Sigman, M. S. Sanford, *J. Am. Chem. Soc.* **2019**, *141*, 15301–15306.
[8] C. S. Sevov, D. P. Hickey, M. E. Cook, S. G. Robinson, S. Barnett, S. D. Minteer, M. S. Sigman, M. S. Sanford, *J. Am. Chem. Soc.* **2017**, *139*, 2924–2927.
[9] S. G. Robinson, Y. Yan, K. H. Hendriks, M. S. Sanford, M. S. Sigman, *J. Am. Chem. Soc.* **2019**, *141*, 10171–10176.
[10] K. H. Hendriks, S. G. Robinson, M. N. Braten, C. S. Sevov, B. A. Helms, M. S. Sigman, S. D. Minteer, M. S. Sanford, *ACS Cent. Sci.* **2018**, *4*, 189–196.
[11] R. M. Darling, K. G. Gallagher, J. A. Kowalski, S. Ha, F. R. Brushett, *Energy Environ. Sci.* **2014**, *7*, 3459–3477.
[12] M. Ue, K. Ida, S. Mori, *J. Electrochem. Soc.* **1994**, *141*, 2989.
[13] J. Volke, V. Skála, *J. Electroanal. Chem.* **1972**, *36*, 383–388.
[14] O. R. Brown, R. J. Butterfield, *Electrochim. Acta* **1982**, *27*, 1647–1653.
[15] R. A. Petersen, D. H. Evans, *J. Electroanal. Chem.* **1987**, *222*, 129–150.

[16] P. H. Rieger, I. Bernal, W. H. Reinmuth, G. K. Fraenkel, *J. Am. Chem. Soc.* **1963**, *85*, 683–693.
[17] R. B. Morris, K. F. Fischer, H. S. White, *J. Phys. Chem.* **1988**, *92*, 5306–5313.
[18] N. A. Macías-Ruvalcaba, D. H. Evans, *J. Electroanal. Chem.* **2011**, *660*, 243–246.
[19] X. Xing, Q. Liu, W. Xu, W. Liang, J. Liu, B. Wang, J. P. Lemmon, *ACS Appl. Energ. Mater.* **2019**, *2*, 2364–2369.
[20] V. V. Pavlishchuk, A. W. Addison, *Inorg. Chim. Acta* **2000**, *298*, 97–102.
[21] A. L. Speelman, J. G. Gillmore, *J. Phys. Chem. A* **2008**, *112*, 5684–5690.
[22] E. J. Lynch, A. L. Speelman, B. A. Curry, C. S. Murillo, J. G. Gillmore, *J. Org. Chem.* **2012**, *77*, 6423–6430.
[23] L. G. Gagliardi, C. B. Castells, C. Ràfols, M. Rosés, E. Bosch, *J. Chem. Eng. Data* **2007**, *52*, 1103–1107.
[24] N. H. Attanayake, J. A. Kowalski, K. V. Greco, M. D. Casselman, J. D. Milshtein, S. J. Chapman, S. R. Parkin, F. R. Brushett, S. A. Odom, *Chem. Mater.* **2019**, *31*, 4353–4363.
[25] C. Zhang, Z. Niu, Y. Ding, L. Zhang, Y. Zhou, X. Guo, X. Zhang, Y. Zhao, G. Yu, *Chem* **2018**, *4*, 2814–2825.
[26] X. Wei, W. Xu, J. Huang, L. Zhang, E. Walter, C. Lawrence, M. Vijayakumar, W. A. Henderson, T. Liu, L. Cosimbescu, B. Li, V. Sprenkle, W. Wang, *Angew. Chem. Int. Ed.* **2015**, *54*, 8684–8687; *Angew. Chem.* **2015**, *127*, 8808–8811.
[27] W. Duan, J. Huang, J. A. Kowalski, I. A. Shkrob, M. Vijayakumar, E. Walter, B. Pan, Z. Yang, J. D. Milshtein, B. Li, C. Liao, Z. Zhang, W. Wang, J. Liu, J. S. Moore, F. R. Brushett, L. Zhang, X. Wei, *ACS Energy Lett.* **2017**, *2*, 1156–1161.

Manuscript received: July 8, 2022
Accepted manuscript online: September 26, 2022
Version of record online: October 27, 2022